Available online at www.sciencedirect.com
SCIENCE DIRECT®
Journal of Nuclear Materials 321 (2003) 288–293
journal of nuclear materials
www.elsevier.com/locate/jnucmat

Effect of MX type particles on creep strength of ferritic steel

M. Tamura [a,*], H. Sakasegawa [b], A. Kohyama [b], H. Esaka [a], K. Shinozuka [a]

[a] Department of Materials Science and Engineering, National Defense Academy of Japan, 1-10-20 Hashirimizu, Yokosuka 239-8686, Japan
[b] Institute of Advanced Energy, Kyoto University, Uji 611-0011, Japan

Received 14 February 2003; accepted 27 May 2003

Abstract

Creep rupture strength at 650 °C and microstructures of the plain ferritic steels with fine particles of the NaCl type (MX) were studied. Precipitation hardening by the fine MX type particles is more effective than solid solution hardening by tungsten. Excess precipitation of MX type particles relatively weakens the grain boundaries as compared with the matrix and, as a consequence, lowers the rupture strength. The equivalent obstacle spacing for mobile dislocations is calculated from the rupture data and is comparable to the interparticle distance observed by transmission electron microscopy. By controlling the interparticle distance of MX type particles with some adjustments of the chemical composition to meet the engineering requirements, it is feasible to develop a new alloy with high rupture strength at 650 °C which is superior to the conventional ferritic steels.

1. Introduction

Structural materials with high creep resistance are necessary for the construction of fusion reactors. Besides this, a requirement for reducing the induced activation makes oxide dispersion strengthened (ODS) ferritic steels attractive [1]. However, one of the drawbacks of the ODS alloys as structural material is the high cost. Therefore, a high strength heat resisting steel which can be manufactured by a conventional method is desirable. Based on such backgrounds, a lot of work to develop an excellent ferritic steel for use in the first wall of TOKAMAK reactors [2] and power stations has been done [3]. However, the final conclusion has not yet been obtained. Moreover, in general, the extension of useful and fundamental knowledge to develop heat resisting steels with high strength is not sufficient.

Among the strengthening mechanisms, precipitation hardening is most reliable in developing heat resisting steels [4]. Among the precipitates carbonitrides of MX type are usually extremely fine and stable in ferrite for a long time [5–7], and these fine particles are expected to increase the creep rupture strength. Therefore, the effect of MX particles on the creep rupture properties of ultra low carbon steel without usual elements such as chromium and vanadium has been preliminarily and basically studied.

2. Experimental procedure

Four experimental alloys with chemical compositions listed in Table 1 were melted in a 10 kg vacuum induction furnace. The ingots were hot-rolled to 12 mm thickness, where the final pass was made at 1000 °C. FETA1 is a low-carbon steel and is a reference material. The second and third alloys are designed to contain TaN (FETA2) and TaC (FETA3) particles, respectively. FETA4 is intended to contain a small amount of W. According to Thermo-Calc, a calculation system of thermodynamic data [8], any compound such as Laves phases, WC and Fe_3C is not precipitated in FETA4 at the test temperature for creep rupture of about 650 °C.

* Corresponding author. Tel.: +81-46 841 3810x3650; fax: +81-46 844 5910.
E-mail address: mtamura@nda.ac.jp (M. Tamura).

0022-3115/$ - see front matter © 2003 Elsevier B.V. All rights reserved.
doi:10.1016/S0022-3115(03)00281-2

Table 1
Chemical composition (mass%), na.: not analysed and bal.: balance

Alloy	C	Si	Mn	P	S	Al	Ta	W	N	O	Fe
FETA1	0.0031	0.0080	0.076	<0.002	0.0010	0.020	na.	na.	0.0019	0.0010	bal.
FETA2	0.0028	0.0080	0.074	<0.002	0.0007	0.030	0.093	na.	0.0130	0.0011	bal.
FETA3	0.016	0.0080	0.090	<0.002	0.0007	0.022	0.17	na.	0.0020	0.0013	bal.
FETA4	0.0026	0.0770	0.092	<0.002	0.0011	0.027	na.	0.031	0.0018	0.0010	bal.

The hot-rolled plates were normalized at 1000 °C for FETA1 and FETA4 and at 1200 °C for FETA2 and FETA3. TaN and TaC are dissolved in the matrix at these temperatures [9]. In order to complete the precipitation of MX type particles and to relieve residual stresses, all of the experimental alloys were aged at 650 °C for 500 h before testing.

Creep rupture tests were performed in air at around 650 °C under a constant load. TEM discs of the typical ruptured specimens were taken from the uniformly deformed portion. Thin films were prepared in 2% perchloric acid–methanol using a single jet polishing apparatus. TEM observations were conducted on a JEOL JEM-2010 operated at 200 kV. Precipitated phases were extracted using a 5% hydrochloric acid–methanol electrolyte. The extracted residues were quantified gravimetrically and identified by an X-ray diffractometer (XRD).

3. Experimental results

3.1. Microstructure

The microstructures of the experimental alloys are full ferrite and the grain size is medium as shown in Table 2. The amount of the extracted residues and the results of XRD are also listed in the table. Major peaks of XRD are identified as MX type particles and some minor peaks are also observed, but they were not successfully identified. The amounts of the residues are larger than the calculated values assuming all of Ta forms stoichiometrical MX precipitates. However, the ratio of the residues of FETA2 and FETA3 is roughly equal to the ratio of the Ta content. These facts indicate that most of Ta is precipitated as TaN (FETA2) or TaC (FETA3) and that precipitates other than MX type particles are few. Vickers hardness numbers are also shown in Table 2, which indicates that the hardness number is increasing with the increase in the amount of precipitated type particles.

Fig. 1 shows the TEM micrographs of ruptured specimens of FETA2 (a) and FETA3 (b). The average particle size and the interparticle distance are measured using the micrographs and the results are listed in Table 2. The interparticle distance is calculated as the average linear intercept on the micrographs. The films are thin enough, about 80 nm, that the observed interparticle distances are considered to be close to the true values. Two types of precipitates, one major, spherical and fine, and about 10 nm in diameter and the other minor (within about 10%), blocky or platelike and rather coarse, about 40 nm, were observed in both TEM micrographs. The precise structural and compositional analysis of the precipitates was not successful under TEM. Most of the precipitates shown in Fig. 1 are judged as TaN or TaC, because the results of XRD prove that MX particles is the major precipitate. Fig. 1 demonstrates that the interparticle distance of TaC in FETA3 is smaller than that of FETA2, TaN. The shorter interparticle distance in FETA3 coincides with the larger Vickers hardness number as compared with FETA2.

3.2. Creep rupture properties

Fig. 2 shows the stress vs. time to rupture diagram of the experimental alloys. Although usually the logarithm of time to rupture (t_r) is plotted against the logarithm of stress, the stress in Fig. 2 is plotted on a linear scale

Table 2
Microstructure characteristics and hardness of the experimental alloys

Alloy	Grain size (μm)	HV10	Precipitation (mass%)	Major precipitate	Particle size (nm)		Interparticle spacing (nm)
					Fine	Coarse	
FETA1	142	66	trace	None	–	–	–
FETA2	115	99	0.143	TaN	13	56	545
FETA3	107	128	0.305	TaC	7	26	165
FETA4	125	73	trace	None	–	–	–

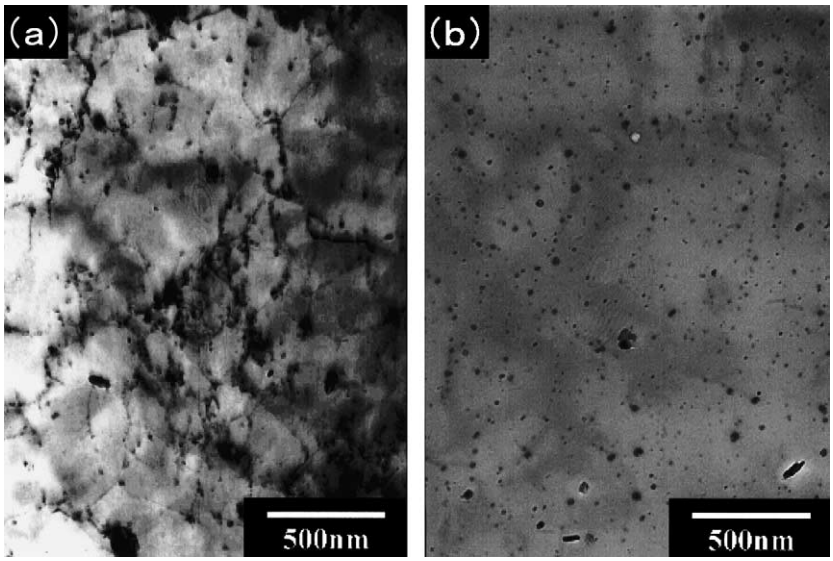

Fig. 1. Transmission electron micrographs of the specimens ruptured at 650 °C and 76.3 MPa (a) FETA2, $t_r = 32.2$ h and (b) FETA3, $t_r = 324.3$ h.

according to a new creep theory [10,11]. According to the new theory, an linear exponential relationship (see Eq. (1)) is established by semi-logarithmic plotting of t_r vs. σ for many heat resistant steels. Rupture data of 8Cr–2WVTa steel [12,13], a pre-IEA heat of F-82H, are also plotted In Fig. 2 for comparison. First, it is found, comparing FETA1 and FETA4, that the effect of solid solution strengthening by W in ferrite is not so remarkable at around 650 °C. On the contrary, t_r of Ta-containing alloys, FETA2 and FETA3, is much longer than that of the reference steel, FETA1. Comparing FETA2 and FETA3, it is reasonable that t_r of FETA3 is longer than that of FETA2 at a high stress level, because the interparticle distance of FETA2 is larger than that of FETA3 as shown in Fig. 1 and Table 2. However, t_r of FETA2 seems to become longer than that of FETA3 at low stress levels. Table 3 shows the results of the creep

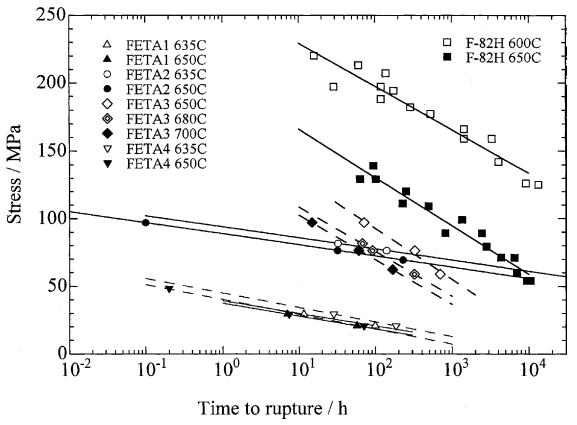

Fig. 2. Stress vs. time-to-rupture diagram of the experimental alloys and F-82H.

Table 3
Results of creep rupture tests

Alloy	T (°C)	Stress (Mpa)	t_r (h)	E_l (%)
FETA 1	635	29.5	11.5	25
	635	20.8	99.0	40
	650	29.5	7.0	53
	650	20.8	57.6	23
FETA 2	635	81.5	32.6	25
	635	76.3	140.0	13
	650	97.1	0.1	37
	650	76.3	32.2	18
	650	69.4	228.4	18
FETA 3	650	97.1	71.4	0.4
	650	76.3	324.3	0.6
	650	59.0	694.0	0.7
	680	81.5	68.1	0.1
	680	76.3	91.8	0.1
	680	59.0	320.0	0.5
	700	97.1	14.8	0.7
	700	76.3	60.8	0.6
	700	62.4	167.0	2.7
FETA 4	635	29.5	28.5	43
	635	20.8	184.3	47
	650	48.5	0.2	43
	650	29.5	7.4	47
	650	20.8	70.8	43

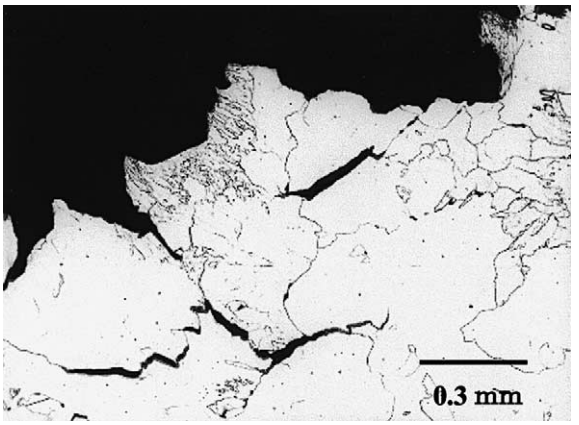

Fig. 3. A longitudinal cross-section view of the ruptured FETA3 at 650 °C and 73.6 MPa.

rupture test. Rupture elongation of FETA3, i.e. about 0.5%, is extremely low as compared with the usual ferritic steels, i.e. about 20%. Fig. 3 shows a longitudinal cross-section view of a rupture specimen of FETA3. Cracks propagate along the grain boundaries, which should be the cause of the shortening or weakening of FETA3.

Extrapolation of the data of FETA2 and F-82H indicates that t_r of FETA2 may exceed that of F-82H at low stress levels, because the slope of the stress vs. time to rupture relation of FETA2 is much smaller than that of F-82H.

4. Discussion

4.1. Extrapolation of rupture data

According to the new creep theory [10], time to rupture, t_r, is expressed by the following equation.

$$t_r = t_{r0} \exp\left(\frac{Q - V\sigma}{RT}\right), \quad (1)$$

where t_{r0}, Q, V, σ, R, T are the pre-exponential factor, activation energy at $\sigma = 0$ (hereinafter, activation energy for simplicity), activation volume, applied stress, the gas constant and absolute temperature, respectively. If the pre-exponential factor is re-written as, $C = -\log t_{r0}$, the constant C corresponds to the well-known Larson–Miller constant [10]. These material constants are calculated by a multiple regression analysis and the results are listed in Table 4. The physical meaning of these material constants is discussed elsewhere [11]. Using these material constants, the rupture stresses for a given t_{r0} can be calculated and the results are also shown in Table 4. Eq. (1) is only valid when $\sigma \geqslant 0.43 \cdot \partial\sigma/\partial \log t_r|_T$ [14]. Therefore, the extrapolated data at low stresses are omitted. It is reconfirmed from the extrapolated rupture stresses that the precipitation hardening by fine MX type particles is remarkably effective. Similar results were reported in an Fe–C–Mo–V–Nb system [15]. F-82H steel is hardened by tempered martensite, $M_{23}C_6$, Laves phase, soluble W, TaC, etc. Among these, the effect of tempered martensite, $M_{23}C_6$ and Laves phase on rupture strength diminishes steeply with the recovery of dislocation structures or the growth of the precipitates, and the effect of soluble W is not so large, as shown in Fig. 2. Therefore, after a long time at 650 °C a major strengthening mechanism should be precipitation hardening by MX type particles. The size of TaC particle changes little even after aging at 650 °C for 30 000 h [5]. The size of TaC in F-82H is just comparable with the experimental alloys, but the amount is about 0.02% at most [5] and much less than the value of FETA2, i.e. 0.1%. Therefore, the rupture strength of FETA2 at a longer time becomes superior to that of F-82H, as shown in Fig. 2 and Tables 3 and 4.

4.2. Interparticle distance of MX type particles

In the previous section it was shown that the rupture strength of F-82H at 650 °C after a long time could be improved by increasing the amount of MX type particles. However, it is well known that in case of precipitation strengthening by undeformed particles the main

Table 4
Material constants of Eq. (1), estimated rupture strength and equivalent obstacle spacing, d/p

Alloy		FETA 1	FETA 2	FETA 3	FETA 4	F-82H
Constant	Q (kJ/mol)	288	840	264	624	661
	V (cm^3/mol)	1862	2137	506	1558	478
	C	12.3	36.8	10.3	31.8	31.9
Rupture strength at 650°C (Mpa)	100 h	18.5	82.7	91.0	17.0	131.6
	1000 h	9.1	74.7	56.2	5.6	94.7
	10 000 h		66.7	21.3		57.8
	100 000 h		58.8			20.9
d/p (μm)		6.18	0.300	240	0.350	0.097

factor to control the rupture strength is not the amount of MX type particles, but the interparticle distance [4]. The authors reported that the obstacle spacing of the commercial heat resisting steels for a mobile dislocation can be calculated using the material constants listed in Table 4, and the calculated values of equivalent obstacle spacing are comparable to the observed TEM values for Cr–Mo steels [11]. The equivalent obstacle spacing, d/p, is given by

$$\frac{d}{p} = \frac{\mu b}{\pi(1-\nu)} \cdot \ln\left(\frac{d}{2r_0}\right) \cdot \frac{V}{Q_{\text{int}}} \tag{2}$$

and

$$Q_{\text{int}} = \frac{Q - Q_d}{(1 - d\ln\mu/d\ln T)}, \tag{3}$$

where d, p, Q_d, μ, b, ν, and r_0 are the spacing of the obstacles, characteristic parameter for the obstacles, activation energy for self-diffusion, shear modulus, length of the Burgers vector, the Poisson's ratio and length between nearest neighbor atoms [11].The value of p is zero, if obstacles do not interact with mobile dislocations and is 1, if obstacles can be assumed to be a single edge dislocation. The equivalent obstacle spacing, d/p, is calculated using Eqs. (2) and (3), and the results are listed in Table 4. In the calculation, d in the logarithm is assumed to be 1 μm, and this assumption is not so sensitive to the calculation of d/p. The calculated value of d/p for FETA2, 300 nm, is comparable to the observed interparticle distance as shown in Table 2, 545 nm, though the value of p is unknown.

Though d/p of FETA3 is much larger than the value of FETA2, the observed interparticle distance is clearly smaller than that of FETA2. Therefore, if the grain boundaries of FETA3 are strengthened by some measures, t_r of FETA3 will be much increased so that d/p of FETA3 should decrease dramatically, because d/p is inversely correlated with the applied stress [11].

4.3. Future development

In our experiment, rupture strength of FETA2 is superior to FETA3. The main reason of this is the intergranular fracture of FETA3. Ohta et al. [16] showed that the continuous precipitation on grain boundaries strongly improved the rupture strength of the austenitic steel. A similar treatment may be possible for the ferritic steel, because $M_{23}C_6$ and Fe_2W are precipitated preferentially on grain boundaries [5].

The results shown in Fig. 1 do not mean that TaN is preferrable to TaC. These results suggest the possibility of finding a new steel which can be manufactured by a conventional method and shows a higher rupture strength than that of F-82H, if we can optimize the shape, size, interparticle distance and amount of the precipitated MX type particles. In order to develop a new alloy, the engineering requirements on weldability, toughness, oxidation, etc. should be also met besides the fundamental studies as mentioned above.

5. Conclusions

The effect of MX type particles in the bcc matrix on the creep rupture strength has been studied fundamentally at around 650 °C, and the following conclusions are obtained:

1. Precipitation hardening by fine MX type particles is extremely effective as compared to solid solution hardening by tungsten.
2. The equivalent obstacle spacing calculated from the rupture data is roughly coincident with the TEM observation.
3. Rupture strength of a plain steel with 0.1% of MX type particles after 10 000 h is estimated to be larger than that of F-82H which is strengthened by the dislocation structure, $M_{23}C_6$, Laves phase and small amounts of MX type particles and solute atoms.

Acknowledgements

The authors wish to express their thanks to Mr T. Kumagaya of Nippon Steel Co. for supplying the experimental alloys. Dr R.W. Olesinski of US Army Material Command is also thanked for his useful advice in arranging this paper.

References

[1] K. Ehrlich, E.E. Bloom, T. Kondo, J. Nucl. Mater. 283–287 (2000) 79.
[2] A. Koyama, Y. Kohno, M. Kuroda, A. Kimura, F. Wan, J. Nucl. Mater. 258–263 (1998) 1319.
[3] F. Masuyama, ISIJ Int. 41 (2001) 612.
[4] V. Foldyna, J. Purmensky, Z. Kubon, ISIJ Int. 41 (Suppl.) (2001) S81.
[5] M. Tamura, K. Shinozuka, H. Esaka, S. Sugimoto, K. Ishizawa, K. Masamura, J. Nucl. Mater. 283–287 (2000) 667.
[6] M. Taneike, K. Kondo, T. Morimoto, ISIJ Int. 41 (Suppl.) (2001) S111.
[7] A. Iseta, H. Teranisi, F. Masuyama, Tetsu-to-Hagane 76 (1990) 1076.
[8] B. Sundman, B. Jansson, J.O. Andersson, CALPHAD 9 (1985) 153.
[9] K. Narita, S. Koyama, Kobe Steel Eng. Rep. 16 (1966) 179.
[10] M. Tamura, H. Esaka, K. Shinozuka, ISIJ Int. 39 (1999) 380.

[11] M. Tamura, H. Esaka, K. Shinozuka, Mater. Trans. JIM 41 (2000) 272.
[12] M. Tamura, H. Hayakawa, M. Tanimura, A. Hishinuma, T. Kondo, J. Nucl. Mater. 141–143 (1986) 1067.
[13] N. Yamanouchi, M. Tamura, H. Hayakawa, A. Hishinuma, T. Kondo, J. Nucl. Mater. 191–194 (1992) 822.
[14] M. Tamura, H. Esaka, K. Shinozuka, Mater. Trans. 44 (2003) 118.
[15] Y. Kadoya, E. Simizu, Tetsu-to-Hagane 85 (1999) 827.
[16] S. Ohta, M. Saori, T. Yoshida, Tetsu-to-Hagane 61 (1975) S694.